



Use of a Ru/Os-CO-diiodide precursor to synthesize heteroleptic 1-alkyl-2-(aryloxy)imidazole complexes: The structural characterization, electrochemistry and catalytic activity

Shyamal Kumar Sarkar¹, Mahendra Sekhar Jana, Tapan Kumar Mondal, Chittaranjan Sinha^{*}

Department of Chemistry, Inorganic Chemistry Section, Jadavpur University, Kolkata 700032, India

ARTICLE INFO

Article history:

Received 30 July 2012

Accepted 5 November 2012

Available online 21 November 2012

Keywords:

Ruthenium and osmium CO-iodide azoimidazoles

X-ray structures

Catalytic oxidation

Electrochemistry

DFT calculations

ABSTRACT

Trans-(I,I)-[M₂(CO)₂(RaaiR')] (M = Ru, Os) (RaaiR' = 1-alkyl-2-(aryloxy)imidazoles) complexes have been synthesized by the reaction of RaaiR' and [Ru(CO)₄I₂] or [Os(CO)₄I₂] in acetonitrile solution and the complexes have been characterized by elemental analysis and spectral (FT-IR, UV-Vis, ¹H NMR) data. The structural confirmation has been determined by single crystal X-ray diffraction of *trans*-(I,I)-[M₂(CO)₂(HaaiEt)] (M = Ru, **3b**; Os, **5b**) (HaaiEt = 1-ethyl-2-(phenyloxy)imidazole) and has shown a distorted octahedral geometry with a *trans*-I,I and *cis*-CO, CO configuration. The complexes show a M(III)/M(II) couple and the reduction of the chelated azoimine ligand. These complexes act as catalysts in the oxidation of PhCH₂OH to PhCHO, 2-butanol (C₄H₉OH) to 2-butanone, cyclopentanol (C₅H₉OH) to cyclopentanone and cyclohexanol to cyclohexanone by N-methylmorpholine-N-oxide (NMO). The molecular orbital diagram has been drawn by density functional theory (DFT) using the optimized geometry from the single crystal X-ray parameters. The assignments of electronic spectra have been carried out by TD-DFT calculations both in the gas and acetonitrile phases.

© 2012 Elsevier Ltd. All rights reserved.

1. Introduction

The metal catalyzed oxidation of primary and secondary alcohols to the corresponding aldehydes and ketones, respectively (Scheme 1), plays an important role in organic synthesis. Catalyses using ruthenium complexes of different heterocyclic-N donor ligands are an active area of present research [1–14]. The catalytic efficiency of ruthenium(II)-carbonyl complexes has been studied using oxidizing agents like H₂O₂, Bu^tOOH and N-methylmorpholine-N-oxide (NMO) [15–18]. The catalytic efficiency of the osmium-carbonyl complexes are relatively less explored than the ruthenium-carbonyl complexes. This may be due to lower catalytic efficiency of osmium complexes because of relativistic effect of the heavier Os(II) than Ru(II).

Azopyridine complexes of ruthenium have been useful in many catalytic reactions, such as hydroformylation, CO₂ reduction, water gas shift reaction [19–24], etc. We have designed 1-alkyl-2-(aryloxy)imidazoles (Scheme 2; HaaiR', **1** and MeaaiR', **2**), a π -acidic chelating azoimine (–N=N=C=N–) ligand [25–29]. The Ru- and Os-carbonyl complexes of these ligands containing M–Cl/M–H bonds (M = Ru, Os) are reported in literature [30–36]. However,

the use of M–I-carbonyl compounds as starting compounds to synthesize polypyridine complexes are rare [37]. The chemical activity of the M–X function (X = halide or pseudohalide) is controlled by the bond strength, the oxidation state of M and the electronic properties of M and X; iodide, being the least electronegative and a highly polarizable halide, may be useful to catalyze different coupling, cross-coupling and oxidation reactions [38]. The catalytic efficiency of a molecule depends on the lability of bonds, chemical oxidation or reduction of the species and the stability of the product(s). In this work, we report the synthesis and characterization of Ru(II)/Os(II)-CO-diiodide complexes of 1-alkyl-2-(aryloxy)imidazoles (RaaiR'). Single crystal X-ray diffraction studies have been undertaken for structural confirmation of the complexes. The electronic structures of the complexes have been calculated by DFT and the TD-DFT methods and have been used to interpret the electronic spectra and redox properties. The catalytic activity of these compounds is examined by the oxidation of primary and secondary alcohols to aldehydes and ketones, respectively, using N-methylmorpholine-N-oxide (NMO).

2. Results and discussion

2.1. Synthesis and formulation

[Ru(CO)₄I₂] and [Os(CO)₄I₂] were used as the starting metal compounds and 1-alkyl-2-(aryloxy)imidazoles (Scheme 2) were

^{*} Corresponding author. Fax: +91 033 2413 7121.

E-mail address: c_r_sinha@yahoo.com (C. Sinha).

¹ Present address: Department of Chemistry, Uluberia College, Uluberia, Howrah 711315, India.

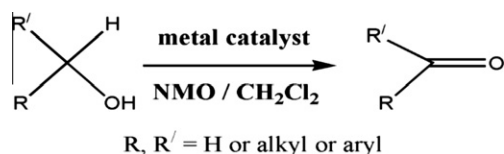
the ligands. A mixture of $[M(CO)_4I_2]$ ($M = Ru, Os$) and the appropriate $RaaiR'$ in acetonitrile under refluxing condition in a dinitrogen atmosphere synthesized dark red solid products. The formulation of the complexes, $[M_2(CO)_2(RaaiR')]$ ($M = Ru$ (**3**, **4**); Os (**5**, **6**)) was supported by microanalytical data. The stereochemical disposition of the donor groups has been confirmed by single crystal X-ray diffraction and shows the two CO ligands are in a *cis*-configuration and the two I^- ligands are bonded in *trans* positions, while $RaaiR'$ (Scheme 2) acts as an N(imidazole) and N(azo) chelator.

The complexes are diamagnetic, indicating the presence of the metal in the +2 oxidation state (d^6). The higher stability of the *trans*-(1,1)-*cis*-(CO, CO) isomer relative to the *cis*-(1,1)-*trans*-(CO, CO) isomer is not surprising due to the *trans* weakening effect of CO.

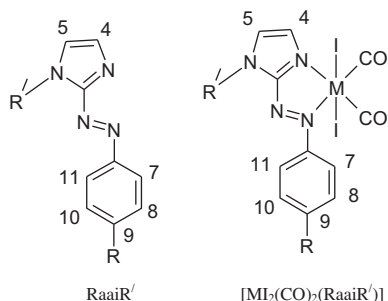
2.2. Infrared and 1H NMR spectral studies

The complexes **3–6** show a sharp stretch at 1993–2003 and 2047–2058 cm^{-1} , corresponding to $\nu(CO)$. The presence of two $\nu(CO)$ stretches refer to a *cis*- $M(CO)_2$ configuration [29]. Infrared spectra of the complexes exhibit $\nu(C=N)$ at 1556–1569 cm^{-1} and $\nu(N=N)$ at 1346–1360 cm^{-1} . The azo ($-N=N-$) stretching is significantly shifted to the lower frequency region compared to the free ligand value (1400–1410 cm^{-1}), which supports efficient $d\pi(Ru) \rightarrow \pi^*(N=N)$ donation in the complexes [25,31–34].

The 1H NMR spectra of the complexes have been recorded in $CDCl_3$ solution and the spectral data are given in Section 3. The spectra were assigned on comparing the spectra of the free ligands, $Ru(II)$ -complexes [25,29] and $Os(II)$ -complexes [35]. The imidazolyl protons, 4- and 5-H, appear as a broad singlet at 7.75–7.85 and 7.45–7.55 ppm, respectively and have been downfield shifted ($\Delta\delta = 0.60$ – 0.80 ppm). The singlet nature of the imidazolyl protons may be due to rapid proton exchange on the NMR timescale with solvent protons (may be coming from moisture during the measurement). The 1-R signals of the chelated ligand appear as follows: 1-Me appears as a singlet at 4.25–4.30 ppm; 1- CH_2-CH_3 gives a quartet (4.55–4.70 ppm, $J = 7.3$ Hz) and a triplet (1.65–1.70 ppm, $J = 7.4$ Hz) respectively; 1- $CH_2-(Ph)$ gives a singlet at 5.70–5.85 ppm. Aryl protons (7-H–11-H) appear at their usual position. The *p*-Me substituent ($MeaaiR'$) shows upper field shifting of



Scheme 1. Catalytic oxidation of secondary alcohols to ketones by NMO.



$R = H$ (**1**), Me (**2**); $R' = Me$ (**a**), Et (**b**) CH_2Ph (**c**); $M = Ru$ (**3**, **4**) and Os (**5**, **6**)

Scheme 2. The ligands and the complexes.

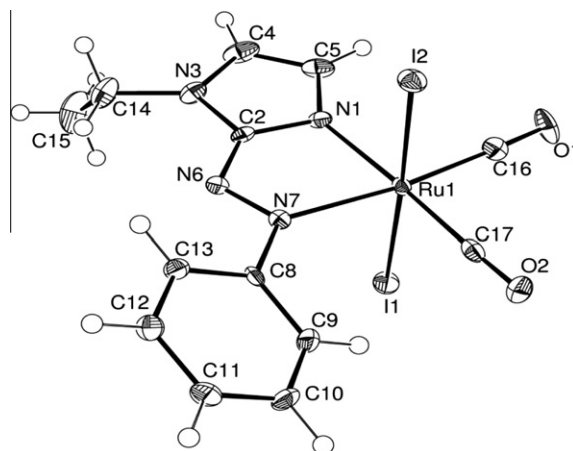


Fig. 1. ORTEP structure of $[Ru_2(CO)_2(HaaiEt)]$ (**3b**) with 35% ellipsoidal probability.

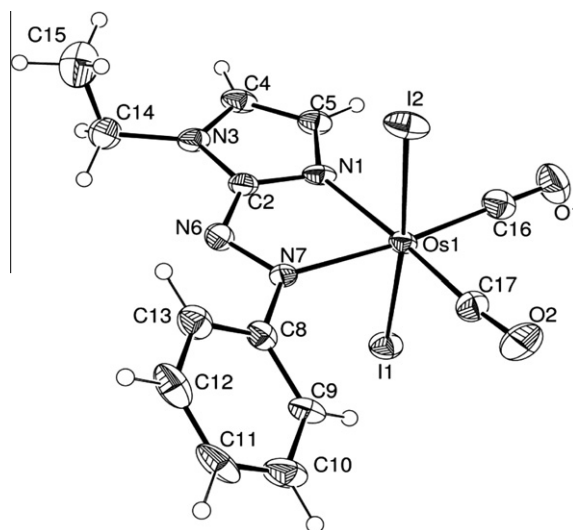


Fig. 2. ORTEP structure $[Os_2(CO)_2(HaaiEt)]$ (**5b**) with 35% ellipsoidal probability.

these protons due to an electron donating effect compared to the phenyl group of $HaaiR'$.

2.3. Molecular structures

The X-ray structures of $[Ru_2(CO)_2(HaaiEt)]$ (**3b**) and $[Os_2(CO)_2(HaaiEt)]$ (**5b**) are shown in Figs. 1 and 2, respectively; selected bond parameters are listed in Table 1. The molecules consist of a central Ru and Os atom surrounded by six coordination centers, and the arrangements are distorted octahedral. The atomic arrangements involve two *trans*-I, two *cis*-CO and a chelated 1-ethyl-2-(phenylazo)imidazole ($HaaiEt$) ligand within the $M_2C_2N_2$ coordination spheres. The CO groups are located *trans* to the azo-N (N') and imidazole-N (N) coordination. The *trans*-I angle, $I(1)-Ru-I(2)$ and $I(1)-Os-I(2)$ are $177.60(1)$ and $174.78(2)$, respectively, and lie in the range of reported data [19,23–30]. The $N(1)-Ru-N(7)$ and $N(1)-Os-N(7)$ chelate angles are $75.20(9)^\circ$ (**3b**) and $74.60(2)^\circ$ (**5b**). Other angles about Ru and Os define the distorted octahedral geometry.

The $Ru(1)-N(7)$ and $Os(1)-N(7)$ bond distances [$N(7)$ is azo-N], $2.141(2)$ Å (**3b**) and $2.129(5)$ Å (**5b**) are longer than the $Ru(1)-N(1)$ and $Os(1)-N(1)$ bond distances [$N(1)$ is imidazole-N, $2.095(2)$ Å (**3b**) and $2.090(5)$ Å (**5b**)] in complexes **3b** and **5b**. In general, the $Ru-N(azo)$ bond distance is shorter than the

Table 1

Selected bond distances (Å) and bond angles (°) for [Ru₂(CO)₂(HaaiEt)] (**3b**) and [Os₂(CO)₂(HaaiEt)] (**5b**).

	[Ru ₂ (CO) ₂ (HaaiEt)] (3b)		[Os ₂ (CO) ₂ (HaaiEt)] (5b)	
	X-ray	DFT/B3LYP	X-ray	DFT/B3LYP
Bond distances (Å)				
M(1)–I(1)	2.698(3)	2.791	2.711(8)	2.785
M(1)–I(2)	2.699(2)	2.788	2.705(9)	2.778
M(1)–N(1)	2.095(3)	2.117	2.090(5)	2.135
M(1)–N(7)	2.141(2)	2.182	2.129(5)	2.167
M(1)–C(16)	1.890(4)	1.891	1.894(8)	1.905
M(1)–C(17)	1.887(4)	1.894	1.856(8)	1.902
C(16)–O(1)	1.127(4)	1.150	1.100(10)	1.153
C(17)–O(2)	1.135(4)	1.151	1.155(10)	1.154
N(6)–N(7)	1.281(3)	1.283	1.286(8)	1.284
Bond angles (°)				
N(1)–M(1)–N(7)	75.21(9)	74.91	74.60(2)	74.01
N(1)–M(1)–C(16)	95.09(1)	94.57	98.50(3)	95.82
N(1)–M(1)–C(17)	175.41(1)	175.0	172.60(3)	172.9
N(1)–M(1)–I(1)	89.93(7)	89.88	88.15(2)	88.79
N(1)–M(1)–I(2)	89.35(7)	88.29	87.52(2)	87.72
N(7)–M(1)–C(16)	170.13(1)	169.4	173.00(2)	169.7
N(7)–M(1)–C(17)	100.68(1)	100.8	99.00(3)	99.05
N(7)–M(1)–I(1)	87.98(6)	88.69	88.82(15)	90.64
N(7)–M(1)–I(2)	89.63(6)	89.11	86.22(15)	87.65
C(16)–M(1)–C(17)	89.08(1)	89.72	87.9(3)	91.06
C(16)–M(1)–I(1)	90.26(9)	90.23	91.1(2)	90.57
C(16)–M(1)–I(2)	92.07(9)	91.69	92.4(2)	90.53
C(17)–M(1)–I(1)	91.99(9)	92.60	95.6(2)	92.62
C(17)–M(1)–I(2)	88.57(9)	89.08	88.4(2)	90.73
I(1)–M(1)–I(2)	177.60(5)	177.4	174.78(2)	176.4
M(1)–C(16)–O(1)	177.2(3)	177.4	179.1(7)	177.0
M(1)–C(17)–O(2)	178.1(3)	177.9	174.1(7)	179.3

Ru–N(imidazole) bond length [25,29–32]. The –N=N– bond length is 1.283(3) and 1.286(6) Å in **3b** and **5b**, respectively which are longer than the free ligand azo distance, 1.267(3) Å [39]. The elongation of the azo bond in complexes is due to extensive $d\pi(\text{Ru}) \rightarrow \pi^*(\text{N}=\text{N})$ donation. The Ru–C bond lengths of **3b** are Ru(1)–C(16), 1.890(4), slightly longer, and Ru(1)–C(17), 1.887(4) Å which is slightly shorter than the Ru–C bond lengths of *trans*-Cl₂[Ru(CO)₂Cl₂(HaaiEt)] [23] ((Ru(1)–C(1), 1.879(3); Ru(1)–C(2), 1.894(3) Å). The two Os–C bond lengths of **5b** differ significantly: Os(1)–C(16), 1.894(8); Os(1)–C(17), 1.856(8) Å. The C–O distances (C(16)–O(1), 1.127(4) (**3b**) and 1.100(10) (**5b**); C(17)–O(2), 1.135(4) (**3b**) and 1.155(10) (**5b**) Å) are different than those of the previously reported data [23]. This may be due to the effect of the Ru–I function where I delocalizes more charge density than Cl in Ru–Cl of *trans*-Cl₂[Ru(CO)₂Cl₂(HaaiEt)] [23]. The pendant phenyl ring is inclined to the mean plane of the chelate ring by 24.57(12)° (**3b**) and 33.26(8)° (**5b**).

DFT calculations on these two molecules were carried out and the optimized geometries of these compounds agree well with the experimentally determined metric parameters (Table 1). The calculations show that the energy of the HOMO of *trans*-(I,I)-[Ru₂(CO)₂(HaaiEt)] (**3b**) (E(HOMO): –5.79 eV) is lower than that of *cis*-(I,I)-[Ru₂(CO)₂(HaaiEt)] (E(HOMO): –4.82 eV) and *cis*-(I,I)-[Os₂(CO)₂(HaaiEt)] (E(HOMO): –5.16 eV). Similarly, the energy of the HOMO of *trans*-(I,I)-[Os₂(CO)₂(HaaiEt)] (**5b**) (E(HOMO): –5.74 eV) is lower than that of *cis*-(I,I)-[Os₂(CO)₂(HaaiEt)] (E(HOMO): –4.80 eV) and *cis*-(I,I)-[Os₂(CO)₂(HaaiEt)] (E(HOMO): –5.14 eV). This reflects the better stability of the *trans*-(I,I) than *cis*-(I,I) configuration, which may be the reason for the isolation of *trans*-(I,I)-[M₂(CO)₂(RaaiR')]. The structural agreement between theory and experiment is satisfactory (Table 1).

2.4. DFT calculations and NBO analyses

Natural bond orbital analyses of **3b** and **5b** have been carried out on the DFT optimized geometry to understand the metal car-

bonyl bonding in the complexes. The NBOs of C–O and M–C are three and one, respectively. The Ru–C and the Os–C bond orbitals are polarized towards the carbon atom, and the C–O bond orbitals are polarized towards the oxygen. The occupancies and hybridization of the C–O and M–C bonds are summarized in the Supplementary data (Table S1). The highly populated anti-bonding NBOs (0.308–0.318 in **3b** and 0.299–0.312 in **5b**) indicate the higher extent of $d\pi(\text{M}) \rightarrow \pi^*(\text{CO})$ (where M = Ru and Os) donation. Increase in back donation decreases the C–O bond strength which means lowering of $\nu(\text{CO})$. It is indeed observed. The calculated electron populations on the 4d orbitals of Ru and 5d orbitals of Os are 7.60 and 7.42 for **3b** and **5b**, respectively. The NBO charge of the Ru and Os atoms are –0.096 and +0.022 in **3b** and **5b** respectively. The charge on the carbonyl carbon is positive (+0.672 in **3b** and +0.626 in **5b**), while that on the oxygen atom is negative (–0.431 in **3b** and –0.435 in **5b**) (Supplementary data, Table S2).

Selected molecular orbitals, along with the energy and composition, of **3b** and **5b** have been summarized as Supplementary data in Tables S3 and S4, respectively. The higher energy occupied orbitals, HOMO and HOMO–1, have 74–83% iodine $p\pi$ character along with a small contribution from metal d -orbitals. HOMO–2 to HOMO–6 have either iodine $p\pi$ and/or $\pi(\text{HaaiEt})$ character. The metal d -orbital contribution (45–70%) has been found in HOMO–7 to HOMO–9 molecular orbitals. The LUMO of the complexes has 87–91% HaaiEt character. The azo function in HaaiEt contributes 48–50% to its composition. The HOMO–LUMO energy gap in the complexes is 2.31 and 2.22 eV in **3b** and **5b**, respectively. LUMO+1 has mixed metal $d\pi$ and iodine $p\pi$ character. LUMO+2 and LUMO+3 show a high mixing of metal $d\pi$ and $\pi^*(\text{CO})$ orbitals (Fig. 3 and Supplementary materials Figs. S1 and S2).

2.5. Electronic transitions and TD DFT calculations

The electronic absorption spectra were measured at room temperature in acetonitrile, and the experimental absorption bands are assigned using the singlet–singlet vertical excitations calculated by the TD-DFT/CPCM method. Absorption spectra of the representative complexes **3b** and **5b** in acetonitrile are shown in Fig. 4. Some of the calculated excitation wavelengths and their assignments are given in Table 2 for **3b** and **5b**. A low energy weak band at 517 and 546 nm has been observed for **3b** and **5b** respectively, which corresponds to $d\pi(\text{M})/p\pi(\text{I}) \rightarrow \pi^*(\text{HaaiEt})$ transitions. The intense sharp band at 405–420 nm in the complexes corresponds to mixed $\pi(\text{HaaiEt}) \rightarrow \pi^*(\text{HaaiEt})$ and $p\pi(\text{I}) \rightarrow \pi^*(\text{HaaiEt})$ charge transfer transitions, while the moderately intense band at 280–310 nm is from purely intra-ligand $\pi(\text{HaaiEt}) \rightarrow \pi^*(\text{HaaiEt})$ transitions.

2.6. Electrochemistry

The complexes **3–6** show one quasi-reversible, 1.44–1.49 V (ΔE , 110–120 mV), and one irreversible, 0.63–0.67 V, oxidative response positive to the reference Ag/AgCl electrode, along with one reversible reductive response, –(0.52–0.56) V (ΔE , 84–90 mV), and one irreversible, –(1.34–1.45) V, cathodic peak when scanned in the negative potential range (Fig. 5 and Table 3).

The redox couples have been assigned on the basis of the DFT results. The HOMO and HOMO–1 of **3b** has 15–18% Ru character and 80–83% iodine contribution, whereas **5b** has 17–22% Os character and 74–79% iodine contribution. So, the first irreversible oxidation of the cyclic voltammogram of the complexes **3–6** has been assigned to the $\text{I}^-/\frac{1}{2}\text{I}_2$ oxidation and the quasi-reversible second oxidation at higher potential range is the M(II)/M(III) couple. The LUMOs of the complexes exclusively have ligand character with 47–50% azo contribution; so the reductions are taking place on the azo function in all the complexes, leading to the formation of the radical anion (RaaiR'^{•–}) and RaaiR'^{2–}.

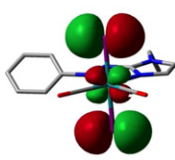
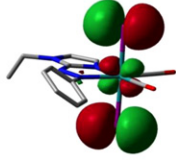
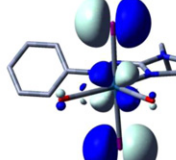
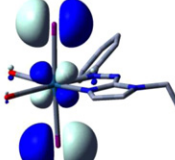
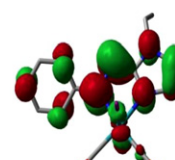
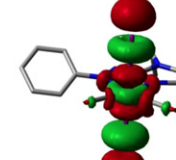
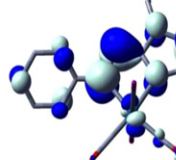
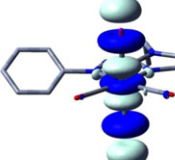
			
E = -5.79 eV; Ru, 18%; I, 80%	E = -5.84 eV; Ru, 15%; I, 83%	E = -5.74 eV; Os, 22%; I, 74%	E = -5.81 eV; Os, 17%; I, 79%
HOMO	HOMO-1	HOMO	HOMO-1
			
E = -3.48 eV; Ru, 03%; I, 05%; HaaiEt, 91%	E = -1.97 eV; Ru, 48%; I, 43%; HaaiEt, 04%	E = -3.52 eV; Os, 04%; I, 05%; HaaiEt, 87%; CO, 04%	E = -1.69 eV; Os, 47%; I, 46%; HaaiEt, 03%; CO, 04%
LUMO	LUMO+1	LUMO	LUMO+1
[RuI ₂ (CO) ₂ (HaaiEt)] (3b)		[OsI ₂ (CO) ₂ (HaaiEt)] (5b)	

Fig. 3. Contour plots of some selected molecular orbitals of [RuI₂(CO)₂(HaaiEt)] (**3b**) and [OsI₂(CO)₂(HaaiEt)] (**5b**).

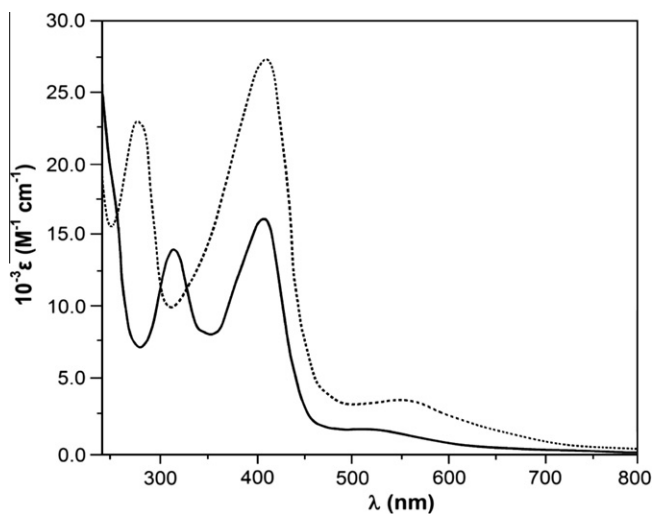


Fig. 4. UV-Vis spectra of [RuI₂(CO)₂(HaaiEt)] (**3b**) (—) and [OsI₂(CO)₂(HaaiEt)] (**5b**) (.....) in acetonitrile.

2.7. Catalytic oxidation of alcohols

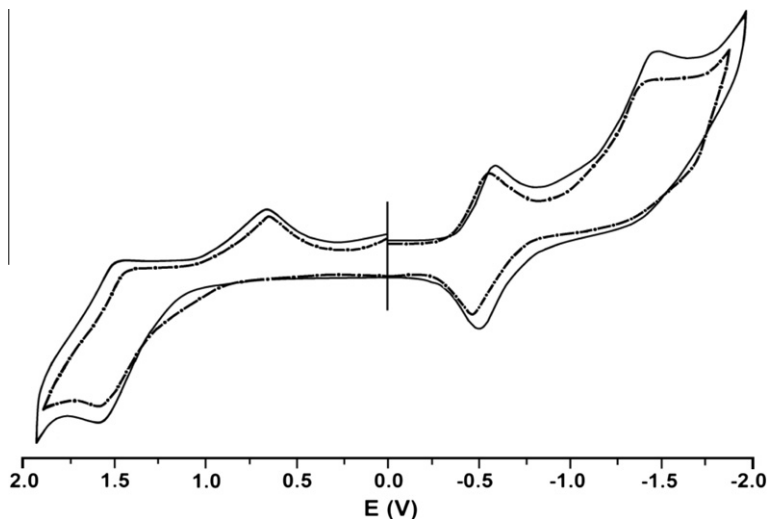
Primary and secondary alcohols are oxidized to aldehydes and ketones, respectively, and these reactions have been studied in the presence of NMO as an oxidant in the presence of [M₂(CO)₂(-RaaiR')]. A typical reaction using the ruthenium and osmium complexes as catalysts and benzyl alcohol, 2-butanol, cyclopentanol and cyclohexanol as substrates at a 1:100 molar ratio is detailed in Section 3 (see below). The reaction has been carried out in CH₂Cl₂ under refluxing conditions for an appropriate period of time. The complexes catalyze the oxidation of PhCH₂OH to PhCHO, C₄H₉OH to C₄H₇O (2-butanone), C₅H₉OH to C₅H₈O (cyclopentanone) and CyCH₂OH to CyC=O (cyclohexanone) with high yields. The ether extracts were evaporated to give the aldehydes/ketones, which were

immediately analyzed by GC. The aldehyde or ketone formed after 2 h of reflux was determined by GC and there was no detectable oxidation in the absence of the ruthenium complex. The results of the investigation suggest that the complexes are able to react efficiently with NMO to yield a high valent ruthenium/osmium-oxo species [10–15], which is capable of oxygen atom transfer to the alcohols. The oxidation ability of cyclopentanol and cyclohexanol are better than benzyl alcohol and 2-butanol. The residue obtained by evaporation of the resultant solution to dryness, had shown a band at 861 and 820 cm⁻¹, characteristic of Ru(IV)=O and Os(IV)=O species, respectively. The catalytic efficiency of [RuI₂(CO)₂(RaaiR')] is higher than that of [OsI₂(CO)₂(RaaiR')], which can be explained in terms of the relativistic effects of the 4d and 5d orbitals [40], the M–CO bond energies and the stability of the M(IV)=O intermediates. Because of a relativistic effect, the 5d orbital of osmium becomes larger in size; hence the interelectronic repulsion in this orbital is reduced, unlike the 4d orbital of ruthenium. The oxidized catalyst M(IV)=O may be more stable in the case of osmium compared to ruthenium and the rate of alcohol oxidation using **3b** as the catalyst could be more favorable than that using **5b**. The 5d orbitals of Os (**5b**) are not sufficiently stabilized, compared to the 4d orbitals of Ru in **3b** (E_{HOMO} (Os-complex, **5b**), -5.74 eV and E_{HOMO} (Ru-complex, **3b**), -5.79 eV).

The role of the M–X (X = Cl, I) function to control the catalytic efficiency of [M₂(CO)₂(RaaiR')] has been examined with reference to ruthenium complexes and the results are compared with [RuCl₂(-CO)₂(HaaiMe/HaaiEt)] (Table 4). It is calculated that the rate of oxidation of PhCH₂OH → PhCHO is higher for the reaction with [RuCl₂(CO)₂(HaaiR')] compared to [RuI₂(CO)₂(HaaiR')]. These two complexes have only difference of the Ru–Cl versus Ru–I bonds. The Ru–I bond (bond distances 2.698(3) and 2.699(2) Å) is longer than Ru–Cl (2.3798(8) and 2.3852(9) Å) [23] so we may apprehend a better lability of the Ru–I bonds. Because of the higher electropositive character of iodide than chloride, the oxidant may be consumed by iodide for some self oxidation reaction and this may be responsible for the low percentage conversion.

Table 2Calculated singlet–singlet vertical electronic transitions for $[\text{RuI}_2(\text{CO})_2(\text{HaaiEt})]$ (**3b**) and $[\text{OsI}_2(\text{CO})_2(\text{HaaiEt})]$ (**5b**).

Excited state	Energy (eV)	λ_{theo}	f	Key transitions	Character
$[\text{RuI}_2(\text{CO})_2(\text{HaaiEt})]$ (3b)					
1	1.940	638.9	0.0033	(97%)HOMO \rightarrow LUMO	$\text{Ru}(d\pi)/\text{I}(p\pi) \rightarrow \text{HaaiEt}(\pi^*)$
2	2.024	612.6	0.0077	(96%)HOMO–1 \rightarrow LUMO	$\text{Ru}(d\pi)/\text{I}(p\pi) \rightarrow \text{HaaiEt}(\pi^*)$
3	2.366	523.9	0.0030	(93%)HOMO–2 \rightarrow LUMO	$\text{I}(p\pi) \rightarrow \text{HaaiEt}(\pi^*)$
7	2.855	434.1	0.3551	(64%)HOMO–4 \rightarrow LUMO	$\text{HaaiEt}(\pi)/\text{I}(p\pi) \rightarrow \text{HaaiEt}(\pi^*)$
8	3.029	409.3	0.1446	(72%)HOMO–5 \rightarrow LUMO	$\text{HaaiEt}(\pi)/\text{I}(p\pi) \rightarrow \text{HaaiEt}(\pi^*)$
13	3.615	342.9	0.0654	(76%)HOMO–6 \rightarrow LUMO	$\text{HaaiEt}(\pi) \rightarrow \text{HaaiEt}(\pi^*)$
17	3.819	324.5	0.0516	(72%)HOMO–10 \rightarrow LUMO	$\text{HaaiEt}(\pi) \rightarrow \text{HaaiEt}(\pi^*)$
$[\text{OsI}_2(\text{CO})_2(\text{HaaiEt})]$ (5b)					
1	1.8157	682.8	0.0016	(95%)HOMO \rightarrow LUMO	$\text{Os}(d\pi)/\text{I}(p\pi) \rightarrow \text{HaaiEt}(\pi^*)$
2	1.9893	623.3	0.0230	(92%)HOMO–1 \rightarrow LUMO	$\text{Os}(d\pi)/\text{I}(p\pi) \rightarrow \text{HaaiEt}(\pi^*)$
3	2.4795	500.0	0.0035	(93%)HOMO–2 \rightarrow LUMO	$\text{I}(p\pi) \rightarrow \text{HaaiEt}(\pi^*)$
5	2.9589	419.0	0.3640	(72%)HOMO–4 \rightarrow LUMO	$\text{HaaiEt}(\pi) \rightarrow \text{HaaiEt}(\pi^*)$
9	3.2396	382.7	0.1367	(78%)HOMO–5 \rightarrow LUMO	$\text{I}(p\pi) \rightarrow \text{HaaiEt}(\pi^*)$
11	3.5311	351.1	0.0672	(73%)HOMO–6 \rightarrow LUMO	$\text{HaaiEt}(\pi) \rightarrow \text{HaaiEt}(\pi^*)$
12	3.7750	328.4	0.0601	(74%)HOMO–11 \rightarrow LUMO	$\text{HaaiEt}(\pi) \rightarrow \text{HaaiEt}(\pi^*)$

**Fig. 5.** Cyclic voltammogram of $[\text{RuI}_2(\text{CO})_2(\text{HaaiEt})]$ (**3b**) (—) and $[\text{OsI}_2(\text{CO})_2(\text{HaaiEt})]$ (**5b**) (---) in acetonitrile solution, supporting electrolyte Bu_4NClO_4 (0.1 M), reference electrode Ag/AgCl at a scan rate of 50 mV s^{-1} .**Table 3**Cyclic voltammetric data of $[\text{MI}_2(\text{CO})_2(\text{RaaiR}')] (\mathbf{3-6})$.

Complex	Cyclic voltammetry ^a			
	$E(\text{I}^-/\frac{1}{2}\text{I}_2)^b$ (V)	$E_{1/2}(\text{M}^{\text{II}}/\text{M}^{\text{III}})$ (V) (ΔE_p , mV)	$E_{1/2}(\text{RaaiR}'/\text{RaaiR}'^-)$ (V) (ΔE_p , mV)	$E(\text{RaaiR}'^-/\text{RaaiR}'^{2-})^c$ (V)
3a	0.652	1.477(110)	−0.548(87)	−1.417
3b	0.641	1.488(112)	−0.552(90)	−1.423
3c	0.652	1.481(110)	−0.562(95)	−1.431
4a	0.665	1.462(115)	−0.561(85)	−1.424
4b	0.647	1.457(110)	−0.549(85)	−1.442
4c	0.657	1.459(114)	−0.550(90)	−1.450
5a	0.634	1.445(110)	−0.518(85)	−1.354
5b	0.634	1.442(115)	−0.507(85)	−1.346
5c	0.637	1.437(110)	−0.516(90)	−1.351
6a	0.632	1.414(115)	−0.534(84)	−1.344
6b	0.641	1.424(120)	−0.537(86)	−1.339
6c	0.637	1.417(110)	−0.531(90)	−1.352

^a In acetonitrile solution, supporting electrolyte $[\text{Bu}_4\text{N}](\text{ClO}_4)$ (0.1 M), reference electrode Ag/AgCl , scan rate = 50 mV s^{-1} . $E_{1/2} = 0.5(E_{\text{pa}} + E_{\text{pc}})$ where E_{pa} and E_{pc} are the anodic and cathodic peak potentials, respectively; $\Delta E_p = E_{\text{pa}} - E_{\text{pc}}$.^b Anodic potential.^c Cathodic potential.

Table 4Catalytic oxidation of alcohols by $[Ml_2(CO)_2(RaaiR')]$ ($M = Ru(II)$ (**3**, **4**) and $Os(II)$ (**5**, **6**) using NMO as the co-oxidant.

Complex	Substrate	Product	Yield ^a (%)	Turnover ^b (%)
3a	benzyl alcohol	benzaldehyde	68	68
	2-butanol	2-butanone	73	73
	cyclopentanol	cyclopentanone	80	80
	cyclohexanol	cyclohexanone	82	82
3b	benzyl alcohol	benzaldehyde	70	70
	2-butanol	2-butanone	72	72
	cyclopentanol	cyclopentanone	81	81
	cyclohexanol	cyclohexanone	83	83
3c	benzyl alcohol	benzaldehyde	69	69
	2-butanol	2-butanone	73	73
	cyclopentanol	cyclopentanone	80	80
	cyclohexanol	cyclohexanone	84	84
4a	benzyl alcohol	benzaldehyde	67	67
	2-butanol	2-butanone	71	71
	cyclopentanol	cyclopentanone	76	76
	cyclohexanol	cyclohexanone	81	81
4b	benzyl alcohol	benzaldehyde	66	66
	2-butanol	2-butanone	74	74
	cyclopentanol	cyclopentanone	78	78
	cyclohexanol	cyclohexanone	82	82
4c	benzyl alcohol	benzaldehyde	67	67
	2-butanol	2-butanone	79	79
	cyclopentanol	cyclopentanone	81	81
	cyclohexanol	cyclohexanone	84	84
5a	benzyl alcohol	benzaldehyde	54	54
	2-butanol	2-butanone	59	59
	cyclopentanol	cyclopentanone	63	63
	cyclohexanol	cyclohexanone	65	65
5b	benzyl alcohol	benzaldehyde	51	51
	2-butanol	2-butanone	58	58
	cyclopentanol	cyclopentanone	65	65
	cyclohexanol	cyclohexanone	66	66
5c	benzyl alcohol	benzaldehyde	55	55
	2-butanol	2-butanone	61	61
	cyclopentanol	cyclopentanone	64	64
	cyclohexanol	cyclohexanone	67	67
6a	benzyl alcohol	benzaldehyde	53	53
	2-butanol	2-butanone	60	60
	cyclopentanol	cyclopentanone	65	65
	cyclohexanol	cyclohexanone	66	66
6b	benzyl alcohol	benzaldehyde	51	51
	2-butanol	2-butanone	60	60
	cyclopentanol	cyclopentanone	65	65
	cyclohexanol	cyclohexanone	66	66
6c	benzyl alcohol	benzaldehyde	53	53
	2-butanol	2-butanone	61	61
	cyclopentanol	cyclopentanone	63	63
	cyclohexanol	cyclohexanone	66	66
$[RuCl_2(CO)_2(HaaiMe)]$	benzyl alcohol	benzaldehyde	84	84
	2-butanol	2-butanone	90	90
	cyclopentanol	cyclopentanone	92	92
	cyclohexanol	cyclohexanone	96	96
$[RuCl_2(CO)_2(HaaiEt)]$	benzyl alcohol	benzaldehyde	86	86
	2-butanol	2-butanone	88	88
	cyclopentanol	cyclopentanone	94	94
	cyclohexanol	cyclohexanone	96	96

Substrate (1 mmol); NMO (3 mmol); complex (0.01 mmol); solvent dichloromethane.

^a The yield of product was determined using an Agilent 7890 series Gas chromatography instrument equipped with a flame ionization detector (FID) using a HP-5 column of 30 m length, 0.53 mm diameter and 5.00 μ m film thickness.^b Moles of product per mole of catalyst.

3. Experimental

3.1. Materials and instrumentation

1-Alkyl-2-(phenylazo)imidazole (**1**) and 1-alkyl-2-(*p*-tolylazo)imidazole (**2**) were synthesized following a previously published procedure [25]. $[Ru(CO)_4I_2]$ and $[Os(CO)_4I_2]$ were also

prepared by a reported method [37]. Imidazole and all other organic chemicals and inorganic salts were available from Sisco Research Lab, Mumbai, India. The purification of acetonitrile and preparation of *n*-tetra-butylammonium perchlorate $[n-Bu_4N][ClO_4]$ for the electrochemical work were done as reported before [29]. Dinitrogen was purified by bubbling through an alkaline pyrogallol solution. All other chemicals and solvents were of reagent grade and were

used without further purification. Commercially available SRL silica gel (60–120 mesh) was used for the column chromatography.

Microanalytical data (C, H, N) were collected on a Perkin-Elmer 2400 CHNS/O elemental analyzer. Infrared spectra were taken on a RX-1 Perkin Elmer spectrophotometer with the samples prepared as KBr pellets. UV–Vis spectral studies were performed on a Perkin Elmer Lambda 25 spectrophotometer. ^1H NMR spectra were recorded using a Bruker (AC) 300 MHz FTNMR spectrometer in CDCl_3 . Cyclic voltammetric measurements were carried out using a CH1 Electrochemical workstation. A platinum wire working electrode, a platinum wire auxiliary electrode and Ag/AgCl reference electrode were used in a standard three-electrode configuration. $[\text{nBu}_4\text{N}][\text{ClO}_4]$ was used as the supporting electrolyte in acetonitrile and the scan rate used was 50 mV s^{-1} in acetonitrile under a dinitrogen atmosphere. The reported potentials are uncorrected for junction potentials.

3.2. Synthesis of the complexes

3.2.1. Synthesis of $[\text{Ru}(\text{CO})_2\text{I}_2(\text{HaaiEt})]$ (**3b**)

To 20 ml acetonitrile suspension of $[\text{Ru}(\text{CO})_4\text{I}_2]$ (100 mg, 0.21 mmol), a 15 ml acetonitrile solution of HaaiEt (**1b**) (45 mg, 0.23 mmol) was added in a 1:1 molar ratio and the solution was refluxed for 4 h under a N_2 atmosphere. The color of the solution changed from red to dark red. The solvent was removed under reduced pressure using a rota-evaporator. The dark red dry mass was then dissolved in a minimum volume of CH_2Cl_2 and subjected to chromatographic separation on a silica gel column (60–120 mesh). The red solution was eluted by acetonitrile–benzene (1:9, v/v). Evaporation of the solvent under reduced pressure afforded pure complex **3b**. The yield was 97 mg (74%). The compounds **3a**, **3c**, **4b**, **4b** and **4c** were also synthesized following the same procedure by the reaction of $[\text{Ru}(\text{CO})_4\text{I}_2]$ with **1a**, **1c**, **2a**, **2b** and **2c** respectively under identical reaction conditions. The yields were 66–75%.

Microanalytical data: Calc. for $[\text{RuI}_2(\text{CO})_2(\text{HaaiMe})]$, $\text{C}_{12}\text{H}_{10}\text{N}_4\text{O}_2\text{I}_2\text{Ru}$ (**3a**): C, 24.17; H, 1.69; N, 9.39. Found: C, 24.25; H, 1.63; N, 9.35%. IR data (KBr disc) (cm^{-1}): $\nu(\text{CO})$ 1993, 2047; $\nu(\text{C}=\text{N})$ 1563; $\nu(\text{N}=\text{N})$ 1349. ^1H NMR data in CDCl_3 (ppm): 7.78 (4-H, s), 7.43 (5-H, bs), 4.27 (N-CH₃, bs), 8.04 (7, 11-H, d, $J = 8.0 \text{ Hz}$), 7.60 (8-10-H, m). UV–Vis (CH_3CN) λ_{max} (ϵ , $\text{M}^{-1} \text{ cm}^{-1}$): 310 (13906), 406 (15651), 516 (1602). Calc. for $[\text{RuI}_2(\text{CO})_2(\text{HaaiEt})]$, $\text{C}_{13}\text{H}_{12}\text{N}_4\text{O}_2\text{I}_2\text{Ru}$ (**3b**): C, 23.62; H, 1.98; N, 9.18. Found: C, 23.70; H, 1.89; N, 9.20%. IR data (KBr disc) (cm^{-1}): $\nu(\text{CO})$ 1999, 2058; $\nu(\text{C}=\text{N})$ 1561; $\nu(\text{N}=\text{N})$ 1346. ^1H NMR data in CDCl_3 (ppm): 7.79 (4-H, bs), 7.47 (5-H, bs), 4.64 (N-CH₂-CH₃, q, $J = 7.0 \text{ Hz}$), 1.68 (N-CH₂-CH₃, t, $J = 7.0 \text{ Hz}$), 8.04 (7, 11-H, d, $J = 7.0 \text{ Hz}$), 7.59 (8-10-H, m). UV–Vis (CH_3CN) λ_{max} (ϵ , $\text{M}^{-1} \text{ cm}^{-1}$): 313 (14292), 405 (16449), 517 (1473). Calc. for $[\text{RuI}_2(\text{CO})_2(\text{HaaiCH}_2\text{Ph})]$, $\text{C}_{18}\text{H}_{14}\text{N}_4\text{O}_2\text{I}_2\text{Ru}$ (**3c**): C, 31.01; H, 1.84; N, 8.51. Found: C, 31.07; H, 1.79; N, 8.52%. IR data (KBr disc) (cm^{-1}): $\nu(\text{CO})$ 2001, 2049; $\nu(\text{C}=\text{N})$ 1558; $\nu(\text{N}=\text{N})$ 1351. ^1H NMR data in CDCl_3 (ppm): 7.81 (4-H, bs), 7.48 (5-H, bs), 5.62 (N-CH₂-Ph, s), 8.08 (7, 11-H, d, $J = 7.0 \text{ Hz}$), 7.57 (8-10-H, m). UV–Vis (CH_3CN) λ_{max} (ϵ , $\text{M}^{-1} \text{ cm}^{-1}$): 305 (14254), 408 (15651), 520 (1578). Calc. for $[\text{RuI}_2(\text{CO})_2(\text{MeaaiMe})]$, $\text{C}_{13}\text{H}_{12}\text{N}_4\text{O}_2\text{I}_2\text{Ru}$ (**4a**): C, 25.58; H, 1.98; N, 9.18. Found: C, 25.62; H, 1.99; N, 9.21%. IR data (KBr disc) (cm^{-1}): $\nu(\text{CO})$ 2003, 2053; $\nu(\text{C}=\text{N})$ 1562; $\nu(\text{N}=\text{N})$ 1360. ^1H NMR data in CDCl_3 (ppm): 7.76 (4-H, bs), 7.34 (5-H, bs), 4.25 (N-CH₃, s), 7.95 (7, 11-H, d, $J = 8.0 \text{ Hz}$), 7.38 (8-10-H, d, $J = 9.0 \text{ Hz}$), 2.48 (9-CH₃, s). UV–Vis (CH_3CN) λ_{max} (ϵ , $\text{M}^{-1} \text{ cm}^{-1}$): 314 (14738), 415 (19005), 511 (1702). Calc. for $[\text{RuI}_2(\text{CO})_2(\text{MeaaiEt})]$, $\text{C}_{14}\text{H}_{14}\text{N}_4\text{O}_2\text{I}_2\text{Ru}$ (**4b**): C, 26.93; H, 2.16; N, 8.97. Found: C, 26.88; H, 2.19; N, 8.92%. IR data (KBr disc) (cm^{-1}): $\nu(\text{CO})$ 2000, 2052; $\nu(\text{C}=\text{N})$ 1559; $\nu(\text{N}=\text{N})$ 1357. ^1H NMR data in CDCl_3 (ppm): 7.75 (4-H, bs), 7.43 (5-H, bs), 4.62 (N-CH₂-CH₃, q, $J = 7.0 \text{ Hz}$), 4.67 (N-CH₂-CH₃, t, $J = 8.0 \text{ Hz}$), 7.95 (7, 11-H, d, $J = 8.0 \text{ Hz}$), 7.35 (8, 10-H, d, $J = 8.0 \text{ Hz}$), 2.48 (9-CH₃, s). UV–Vis (CH_3CN): λ_{max} (ϵ , $\text{M}^{-1} \text{ cm}^{-1}$):

314 (11548), 415 (14952), 509 (1715). Calc. for $[\text{RuI}_2(\text{CO})_2(\text{MeaaiCH}_2\text{Ph})]$, $\text{C}_{19}\text{H}_{16}\text{N}_4\text{O}_2\text{I}_2\text{Ru}$ (**4c**): C, 32.11; H, 2.09; N, 8.32. Found: C, 31.92; H, 2.12; N, 5.31%. IR data (KBr disc) (cm^{-1}): $\nu(\text{CO})$ 2002, 2054; $\nu(\text{C}=\text{N})$ 1556; $\nu(\text{N}=\text{N})$ 1352. ^1H NMR data in CDCl_3 (ppm): 7.78 (4-H, bs), 7.45 (5-H, bs), 5.53 (N-CH₂-Ph, s), 7.89 (7, 11-H, d, $J = 8.0 \text{ Hz}$), 7.37 (8, 10-H, d, $J = 8.0 \text{ Hz}$), 2.49 (9-CH₃, s). UV–Vis (CH_3CN) λ_{max} (ϵ , $\text{M}^{-1} \text{ cm}^{-1}$): 310 (13452), 412 (14925), 512 (1625).

3.2.2. Synthesis of $[\text{Os}(\text{CO})_2\text{I}_2(\text{HaaiEt})]$ (**5b**)

Complex **5b** was prepared by the reaction of $[\text{Os}(\text{CO})_4\text{I}_2]$ (100 mg, 0.18 mmol) with HaaiEt (**1b**) (36.02 mg, 0.19 mmol) following the same procedure as for **3b**. Yield was 90.67 mg (72%). Compounds **5a**, **5c**, **6a**, **6b** and **6c** were also synthesized following the same procedure by the reaction of $[\text{Os}(\text{CO})_4\text{I}_2]$ with **1a**, **1c**, **2a**, **2b** and **2c** respectively in the same molar ratio (1:1). The yields were about (64–73)%.

Microanalytical data: Calc. for $[\text{OsI}_2(\text{CO})_2(\text{HaaiMe})]$, $\text{C}_{12}\text{H}_{10}\text{N}_4\text{O}_2\text{I}_2\text{Os}$ (**5a**): C, 21.08; H, 1.47; N, 8.17. Found: C, 21.12; H, 1.46; N, 8.18%. IR data (KBr disc) (cm^{-1}): $\nu(\text{CO})$ 1999, 2051; $\nu(\text{C}=\text{N})$ 1561; $\nu(\text{N}=\text{N})$ 1353. ^1H NMR data in CDCl_3 (ppm): 7.72 (4-H, bs), 7.48 (5-H, bs), 4.30 (N-CH₃, s), 8.06 (7, 11-H, d, $J = 7.0 \text{ Hz}$), 7.63 (8-10-H, m). UV–Vis (CH_3CN) λ_{max} (ϵ , $\text{M}^{-1} \text{ cm}^{-1}$): 287 (21456), 415 (25465), 542 (2945). For $[\text{OsI}_2(\text{CO})_2(\text{HaaiEt})]$, $\text{C}_{13}\text{H}_{12}\text{N}_4\text{O}_2\text{I}_2\text{Os}$ (**5b**): C, 22.30 (22.28); H, 1.73 (1.74); N, 8.00 (7.99). IR data (KBr disc) (cm^{-1}): $\nu(\text{CO})$ 1996, 2050; $\nu(\text{C}=\text{N})$ 1569; $\nu(\text{N}=\text{N})$ 1348. ^1H NMR data in CDCl_3 (ppm): 7.69 (4-H, bs), 7.50 (5-H, bs), 4.66 (N-CH₂-CH₃, q, $J = 7.0 \text{ Hz}$), 1.70 (N-CH₂-CH₃, t, $J = 7.0 \text{ Hz}$), 8.00 (7, 11-H, d, $J = 7.0 \text{ Hz}$), 7.61 (8-10-H, m). UV–Vis (CH_3CN) λ_{max} (ϵ , $\text{M}^{-1} \text{ cm}^{-1}$): 280 (22546), 413 (27401), 546 (3131). Calc. for $[\text{OsI}_2(\text{CO})_2(\text{HaaiCH}_2\text{Ph})]$, $\text{C}_{18}\text{H}_{12}\text{N}_4\text{O}_2\text{I}_2\text{Os}$ (**5c**): C, 27.29; H, 1.62; N, 7.49. Found: C, 27.18; H, 1.62; N, 7.51%. IR data (KBr disc) (cm^{-1}): $\nu(\text{CO})$ 2001, 2048; $\nu(\text{C}=\text{N})$ 1563; $\nu(\text{N}=\text{N})$ 1352. ^1H NMR data in CDCl_3 (ppm): 7.70 (4-H, bs), 7.51 (5-H, bs), 5.57 (N-CH₂-Ph, s), 8.03 (7, 11-H, d, $J = 7.0 \text{ Hz}$), 7.62 (8-10-H, m). UV–Vis (CH_3CN) λ_{max} (ϵ , $\text{M}^{-1} \text{ cm}^{-1}$): 290 (23452), 410 (26125), 540 (2745). Calc. for $[\text{OsI}_2(\text{CO})_2(\text{MeaaiMe})]$, $\text{C}_{13}\text{H}_{12}\text{N}_4\text{O}_2\text{I}_2\text{Os}$ (**6a**): C, 22.30; H, 1.73; N, 8.01. Found: C, 22.29; H, 1.74; N, 8.16%. IR data (KBr disc) (cm^{-1}): $\nu(\text{CO})$ 2002, 2051; $\nu(\text{C}=\text{N})$ 1562; $\nu(\text{N}=\text{N})$ 1360. ^1H NMR data in CDCl_3 (ppm): 7.68 (4-H, bs), 7.47 (5-H, bs), 4.32 (N-CH₃, s), 7.95 (7, 11-H, d, $J = 7.0 \text{ Hz}$), 7.41 (8-10-H, d, $J = 8.5$), 2.47 (9-CH₃, s). UV–Vis (CH_3CN) λ_{max} (ϵ , $\text{M}^{-1} \text{ cm}^{-1}$): 295 (19457), 418 (25134), 537 (2947). Calc. for $[\text{OsI}_2(\text{CO})_2(\text{MeaaiEt})]$, $\text{C}_{14}\text{H}_{14}\text{N}_4\text{O}_2\text{I}_2\text{Os}$ (**6b**): C, 23.54; H, 1.98; N, 7.84. Found: C, 23.49; H, 1.96; N, 7.73%. IR data (KBr disc) (cm^{-1}): $\nu(\text{CO})$ 2003, 2049; $\nu(\text{C}=\text{N})$ 1560; $\nu(\text{N}=\text{N})$ 1353. ^1H NMR data in CDCl_3 (ppm): 7.67 (4-H, bs), 7.45 (5-H, bs), 4.63 (N-CH₂-CH₃, q, $J = 7.0 \text{ Hz}$), 1.67 (N-CH₂-CH₃, t, $J = 8.0 \text{ Hz}$), 7.93 (7, 11-H, d, $J = 7.0 \text{ Hz}$), 7.43 (8, 10-H, d, $J = 9.0 \text{ Hz}$), 2.46 (9-CH₃, s). UV–Vis (CH_3CN) λ_{max} (ϵ , $\text{M}^{-1} \text{ cm}^{-1}$): 287 (21484), 415 (28451), 540 (2871). Calc. for $[\text{OsI}_2(\text{CO})_2(\text{MeaaiCH}_2\text{Ph})]$, $\text{C}_{19}\text{H}_{16}\text{N}_4\text{O}_2\text{I}_2\text{Os}$ (**6c**): C, 28.36; H, 1.85; N, 7.35. Found: C, 28.34; H, 1.84; N, 7.41%. IR data (KBr disc) (cm^{-1}): $\nu(\text{CO})$ 2000, 2051; $\nu(\text{C}=\text{N})$ 1559; $\nu(\text{N}=\text{N})$ 1356. ^1H NMR data in CDCl_3 (ppm): 7.70 (4-H, bs), 7.48 (5-H, bs), 5.55 (N-CH₂-Ph, s), 7.97 (7, 11-H, d, $J = 7.0 \text{ Hz}$), 7.39 (8, 10-H, d, $J = 9.0 \text{ Hz}$), 2.45 (9-CH₃, s). UV–Vis (CH_3CN) λ_{max} (ϵ , $\text{M}^{-1} \text{ cm}^{-1}$): 290 (22154), 412 (27346), 541 (3102).

3.3. X-ray crystal structure analysis

Details of the crystal analyses, data collection and structure refinement data are given in Table 5. Crystal mounting was done on glass fibers with epoxy cement. Single crystal data collections were performed with an automated Bruker SMART APEX CCD diffractometer. Unit cell parameters were determined from least-squares refinement of setting angles with θ in the range $2.40 \leq \theta \leq 25.35^\circ$ (**3b**) and $1.97 \leq \theta \leq 25.98^\circ$ (**5b**). Out of 11177 collected data 3211, number of refined parameters 200, for **3b**

Table 5

Crystal data and details of the structure determination of $[\text{Ru}_2(\text{CO})_2(\text{HaaiEt})]$ (**3b**) and $[\text{Os}_2(\text{CO})_2(\text{HaaiEt})]$ (**5b**).

Compound	$[\text{Ru}_2(\text{CO})_2(\text{HaaiEt})]$ (3b)	$[\text{Os}_2(\text{CO})_2(\text{HaaiEt})]$ (5b)
Formula	$\text{C}_{13}\text{H}_{12}\text{N}_4\text{O}_2\text{I}_2\text{Ru}$	$\text{C}_{13}\text{H}_{12}\text{N}_4\text{O}_2\text{I}_2\text{Os}$
M_r	611.14	700.30
Crystal system	monoclinic	monoclinic
Space group	$P2_1/c$	$P2_1/n$
a (Å)	11.7935(14)	8.283(5)
b (Å)	10.6119(10)	14.348(5)
c (Å)	14.7790(16)	15.098(5)
β (°)	106.318(3)	15.098(5)
Cell volume (Å ³)	1775.1(3)	1774.4(14)
Z	4	4
μ (mm ^{−1})	4.372	10.676
T (K)	93(2)	293(2)
ρ_{calcd} (g cm ^{−3})	2.287	2.622
θ range (°)	2.40–25.35	1.97–25.98
Data/restraints/ parameters	3211/0/200	3414/0/199
R_1^a , wR_2^b [$I > 2\sigma(I)$]	0.0246, 0.0409	0.0370, 0.0892
GOF	1.07	1.03

^a $R = \sum |F_o - F_c| / \sum F_o$.

^b $wR = [\sum w(F_o^2 - F_c^2) / \sum wF_o^4]^{1/2}$ are general but w are different, $w = 1/[\sigma^2(F^2) + (0.0156P)^2]$ for **3b**; $w = 1/[\sigma^2(F^2) + (0.0537P)^2 + 1.1520P]$ for **5b**, where $P = (F_o^2 + 2F_c^2)/3$.

and 25 112 collected data 3414, number of refined parameters 199, for **5b** with $I > 2\sigma(I)$ were used for the structure solution. The hkl ranges are $-19 \leq h \leq 14$, $-10 \leq k \leq 12$, $-17 \leq l \leq 17$ for **3b** and $-10 \leq h \leq 10$, $-17 \leq k \leq 17$, $-18 \leq l \leq 18$ for **5b**. Reflection data were recorded using the ω scan technique. The structures were solved and refined by the full-matrix least-squares techniques on F^2 using the SHELX-97 program [41,42]. The absorption corrections were done by the multi-scan technique. All data were corrected for Lorentz and polarization effects, and the non-hydrogen atoms were refined anisotropically. Hydrogen atoms were constrained to ride on the respective carbon atoms with isotropic displacement parameters equal to 1.2 times the equivalent isotropic displacement of their parent atom in all cases.

3.4. Procedure for catalytic oxidation

Catalytic oxidation of primary and secondary alcohols to the corresponding aldehydes and ketones respectively by ruthenium(II) and osmium(II) carbonyl iodide complexes were studied in the presence of NMO as a co-oxidant and the byproduct, water, was removed by using about 0.5 g of molecular sieves. Typical reactions were carried out using the ruthenium and osmium complexes as the catalyst and benzyl alcohol, 2-butanol, cyclopentanol and cyclohexanol as substrates in a 1:100 molar ratio. Solutions of the ruthenium and osmium complexes (0.01 mmol) in 20 cm³ CH₂Cl₂ were added to a solution of the substrate (1 mmol) and NMO (3 mmol). The solution mixture was refluxed for 2 h and the solvent was then evaporated from the mother liquor under reduced pressure. The residue was then extracted with petroleum ether (20 cm³) and was analyzed by GC using an Agilent 7890 series Gas chromatography instrument equipped with a flame ionization detector (FID) using a HP-5 column of 30 m length, 0.53 mm diameter and 5.00 μm film thickness. The ether extracts were evaporated to give the corresponding aldehydes/ketones, which were then isolated and quantified as their 2,4-dinitrophenylhydrazone derivatives.

3.5. Computational methods

All computations were performed using the GAUSSIAN03 (G03) [43] software. The Becke's three-parameter hybrid exchange func-

tional and the Lee–Yang–Parr non-local correlation functional [44–46] (B3LYP) were used throughout. The 6-31G(d) basis set was used for the C, H, N and O atoms, while the 6-311G(d) basis functions was used for the I atoms [47]. The Lanl2TZ(f) basis set with effective core potentials was employed for the Ru and Os atoms [48]. The vibrational frequency calculations were performed to ensure that the optimized geometries represent the local minima and there are only positive eigen values. Natural bond orbital analyses were performed using the NBO 3.1 module of GAUSSIAN03 [49]. Vertical electronic excitations based on B3LYP optimized geometries were computed for the time-dependent density functional theory (TD-DFT) formalism [50–52] in acetonitrile using a conductor-like polarizable continuum model (CPCM) [50–52]. Gauss Sum [53] was used to calculate the fractional contributions of various groups to each molecular orbital.

4. Conclusion

The reaction of 1-alkyl-2-(phenylazo)imidazole (HaaiR') (**1**) and 1-alkyl-2-(p-tolylazo)imidazole (MeaaiR') (**2**) with $[\text{Ru}(\text{CO})_4\text{I}_2]$ and $[\text{Os}(\text{CO})_4\text{I}_2]$ have isolated the complexes $[\text{M}_2(\text{CO})_2\text{I}_2(\text{RaaiR}')]_2$ in which RaaiR' serve as an N(imidazole), N(azo) bidentate chelator. Single crystal X-ray diffraction has confirmed the structures of the complexes. Cyclic voltammetry shows the M(III)/M(II) redox response, along with ligand reductions. The catalytic activity of the complexes has been examined for the oxidation of benzyl alcohol to aldehyde, 2-butanol to 2-butanone, cyclopentanol to cyclopentanone and cyclohexanol to cyclohexanone using NMO as an oxidant. DFT calculations have been used to explain the spectra and redox properties of the complexes.

Acknowledgments

Financial support from the Department of Science & Technology and University Grants Commission, New Delhi are gratefully acknowledged.

Appendix A. Supplementary data

CCDC 856090 and 804818 contain the supplementary crystallographic data for **3b** and **5b**, respectively. These data can be obtained free of charge via <http://www.ccdc.cam.ac.uk/conts/retrieving.html>, or from the Cambridge Crystallographic Data Centre, 12 Union Road, Cambridge CB2 1EZ, UK; fax: (+44) 1223-336-033; or e-mail: deposit@ccdc.cam.ac.uk.

References

- [1] T. Okumura, S. Watanabe, T. Yagyu, H. Takagi, Y. Fukushima, H. Masuda, K. Jitsukawa, J. Mol. Catal. A: Chem. 307 (2009) 51.
- [2] Z.W. Yang, Q.X. Kang, F. Quan, Z.Q. Lei, J. Mol. Catal. A: Chem. 261 (2007) 190.
- [3] G.-ping Yao, J. Li, Y. Luo, W.-jun Sun, J. Mol. Catal. A: Chem. 361–362 (2012) 29.
- [4] A.J.A. Watson, A.C. Maxwell, J.M.J. Williams, Org. Lett. 11 (2009) 2667.
- [5] Z.Q. Lei, Q.X. Kang, X.Z. Bai, Z.W. Yang, Q.H. Zhang, Chin. Chem. Lett. 16 (2005) 846.
- [6] T. Joseph, S.S. Deshpande, S.B. Halligudi, A. Vinu, S. Ernst, M. Hartmann, J. Mol. Catal. A: Chem. 206 (2003) 13.
- [7] R.A. Sanchez-Delgado, N. Valencia, R.-L. Marquez-Silva, A. Andriollo, M. Medina, Inorg. Chem. 25 (1986) 1106.
- [8] S.K. Sarkar, M.S. Jana, T.K. Mondal, C. Sinha, J. Organomet. Chem. 716 (2012) 129.
- [9] J.H. Dam, G. Osztrovszky, L.U. Nordström, R. Madsen, Chem. Eur. J. 16 (2010) 6820.
- [10] M. Haukka, T. Venalainen, M. Kallinen, T.A. Pakkanen, J. Mol. Catal. A: Chem. 136 (1998) 127.
- [11] K.N. Kumar, R. Ramesh, Y. Liu, J. Mol. Catal. A: Chem. 265 (2007) 218.
- [12] M.U. Raja, N. Gowri, R. Ramesh, Polyhedron 29 (2010) 1175.
- [13] P. Chutia, N. Kumari, M. Sharma, J.D. Woollins, A.M.Z. Slawin, D.K. Dutta, Polyhedron 23 (2004) 1657.
- [14] C.S. Cho, D.Y. Kim, S.C. Shim, Bull. Korean Chem. Soc. 26 (2005) 802.

- [15] M. Haukka, M. Ahlgren, T.A. Pakkanen, J. Chem. Soc., Dalton Trans. (1996) 1927.
- [16] M. Haukka, J. Kiviaho, M. Ahlgren, T.A. Pakkanen, Organometallics 14 (1995) 825.
- [17] D. Choudhury, R.F. Jones, G. Smith, D.J. Cole-Hamilton, J. Chem. Soc., Dalton Trans. (1982) 1143.
- [18] B. Tanaka, B.-C. Tzeng, H. Nagao, S.-M. Pentg, T. Tanaka, Inorg. Chem. 32 (1993) 1508.
- [19] M. Shivakumar, K. Pramanik, P. Ghosh, A. Chakravorty, Inorg. Chem. 37 (1998) 5968.
- [20] M. Shivakumar, K. Pramanik, I. Bhattacharyya, A. Chakravorty, Inorg. Chem. 39 (2000) 4332.
- [21] K. Pramanik, M. Shivakumar, P. Ghosh, A. Chakravorty, Inorg. Chem. 39 (2000) 195.
- [22] Au Yat-Kun, Kung-Kai Cheung, Wing-Tak Wong, Inorg. Chim. Acta 238 (1995) 193.
- [23] Yat Li, Wing-Tak Wong, J. Cluster Sci. 12 (2001) 595.
- [24] Yat Li, Zhen-Yang Lin, Wing-Tak Wong, Eur. J. Inorg. Chem. (2001) 3163.
- [25] T.K. Misra, D. Das, C. Sinha, P.K. Ghosh, C.K. Pal, Inorg. Chem. 37 (1998) 1672.
- [26] T.K. Mondal, J.-S. Wu, T.-H. Lu, Sk. Jasimuddin, C. Sinha, J. Organomet. Chem. 694 (2009) 3518.
- [27] J. Dinda, S. Senapoti, T. Mondal, A.D. Jana, M. Chiang, T.-H. Lu, C. Sinha, Polyhedron 25 (2006) 1125.
- [28] P. Byabartta, Sk. Jasimuddin, G. Mostafa, T.-H. Lu, C. Sinha, Polyhedron 22 (2003) 849.
- [29] T.K. Mondal, S.K. Sarker, P. Raghavaiah, C. Sinha, Polyhedron 27 (2008) 3020.
- [30] T.K. Mondal, J. Dinda, A.M.Z. Slawin, J.D. Woollins, C. Sinha, Polyhedron 26 (2007) 600.
- [31] T. Mathur, J. Dinda, P. Datta, G. Mostafa, T.-H. Lu, C. Sinha, Polyhedron 25 (2006) 2503.
- [32] T.K. Mondal, P. Raghavaiah, A.K. Patra, C. Sinha, Inorg. Chem. Commun. 13 (2010) 273.
- [33] T.K. Mondal, J.-S. Wu, T.-H. Lu, R. Pallepogu, A.K. Patra, Sk. Jasimuddin, C. Sinha, J. Organomet. Chem. 694 (2009) 3518.
- [34] T.K. Mondal, J. Dinda, J. Cheng, T.-H. Lu, C. Sinha, Inorg. Chim. Acta 361 (2008) 2431.
- [35] T.K. Mondal, Joydev Dinda, Alexandra M.Z. Slawin, J. Derek Woollins, C. Sinha, Polyhedron 26 (2007) 600.
- [36] M. Shivakumar, K. Pramanik, P. Ghosh, A. Chakravorty, Chem. Commun. (1998) 2103.
- [37] E.R. Corey, M.V. Evans, L.F. Dahl, J. Inorg. Nucl. Chem. 24 (1962) 926.
- [38] M.A. Fernández-Rodríguez, J.F. Hartwig, J. Org. Chem. 74 (2009) 1663.
- [39] J. Otsuki, K. Suwa, K.K. Sarker, C. Sinha, J. Phys. Chem. A 111 (2007) 1403.
- [40] P. Pyykko, Chem. Rev. 88 (1988) 563.
- [41] M. Sheldrick, SHELXS-97, Program for the Solution of Crystal Structures, University of Gottingen, Germany, 1997.
- [42] G.M. Sheldrick, SHELXL-97, Program for the Refinement of Crystal Structures, University of Gottingen, Germany, 1997.
- [43] M.J. Frisch, G.W. Trucks, H.B. Schlegel, G.E. Scuseria, M.A. Robb, J.R. Cheeseman, J.A. Montgomery Jr., T. Vreven, K.N. Kudin, J.C. Burant, J.M. Millam, S.S. Iyengar, J. Tomasi, V. Barone, B. Mennucci, M. Cossi, G. Scalmani, N. Rega, G.A. Petersson, H. Nakatsuji, M. Hada, M. Ehara, K. Toyota, R. Fukuda, J. Hasegawa, M. Ishida, T. Nakajima, Y. Honda, O. Kitao, H. Nakai, M. Klene, X. Li, J.E. Knox, H.P. Hratchian, J.B. Cross, V. Bakken, C. Adamo, J. Jaramillo, R. Gomperts, R.E. Stratmann, O. Yazyev, A.J. Austin, R. Cammi, C. Pomelli, J.W. Ochterski, P.Y. Ayala, K. Morokuma, G.A. Voth, P. Salvador, J.J. Dannenberg, V.G. Zakrzewski, S. Dapprich, A.D. Daniels, M.C. Strain, O. Farkas, D.K. Malick, A.D. Rabuck, K. Raghavachari, J.B. Foresman, J.V. Ortiz, Q. Cui, A.G. Baboul, S. Clifford, J. Cioslowski, B.B. Stefanov, G. Liu, A. Liashenko, P. Piskorz, I. Komaromi, R.L. Martin, D.J. Fox, T. Keith, M.A. Al-Laham, C.Y. Peng, A. Nanayakkara, M. Challacombe, P.M.W. Gill, B. Johnson, W. Chen, M.W. Wong, C. Gonzalez, J.A. Pople, Gaussian 03, Revision D.01, Gaussian, Inc., Wallingford, CT, 2004.
- [44] A.D. Becke, J. Chem. Phys. 98 (1993) 5648.
- [45] P.J. Stevens, J.F. Devlin, C.F. Chabalowski, M.J. Frisch, J. Phys. Chem. 98 (1994) 11623.
- [46] C. Lee, W. Yang, R.G. Parr, Phys. Rev. B 37 (1988) 785.
- [47] R. Krishnan, J.S. Binkley, R. Seeger, J.A. Pople, J. Chem. Phys. 72 (1980) 650.
- [48] A.W. Ehlers, M. Bohme, S. Dapprich, A. Gobbi, A. Hollwarth, V. Jonas, K.F. Kohler, R. Stegmann, A. Veldkamp, G. Frenking, Chem. Phys. Lett. 208 (1993) 111.
- [49] E.D. Glendening, A.E. Reed, J.E. Carpenter, F. Weinhold, NBO, Version 3.1.
- [50] R. Bauernschmitt, R. Ahlrichs, Chem. Phys. Lett. 256 (1996) 454.
- [51] R.E. Stratmann, G.E. Scuseria, M.J. Frisch, J. Chem. Phys. 109 (1998) 8218.
- [52] M.E. Casida, C. Jamorski, K.C. Casida, D.R. Salahub, J. Chem. Phys. 108 (1998) 4439.
- [53] V. Barone, M. Cossi, J. Phys. Chem. A 102 (1998) 1995.